



## Collective Surfing of Chemically Active Particles

Hassan Masoud<sup>1,2,\*</sup> and Michael J. Shelley<sup>1,†</sup>

<sup>1</sup>*Applied Mathematics Laboratory, Courant Institute of Mathematical Sciences, New York University, New York, New York 10012, USA*

<sup>2</sup>*Department of Mechanical and Aerospace Engineering, Princeton University, Princeton, New Jersey 08544, USA*

(Received 17 December 2013; published 26 March 2014)

We study theoretically the collective dynamics of immotile particles bound to a 2D surface atop a 3D fluid layer. These particles are chemically active and produce a chemical concentration field that creates surface-tension gradients along the surface. The resultant Marangoni stresses create flows that carry the particles, possibly concentrating them. For a 3D diffusion-dominated concentration field and Stokesian fluid we show that the surface dynamics of active particle density can be determined using nonlocal 2D surface operators. Remarkably, we also show that for both deep or shallow fluid layers this surface dynamics reduces to the 2D Keller-Segel model for the collective chemotactic aggregation of slime mold colonies. Mathematical analysis has established that the Keller-Segel model can yield finite-time, finite-mass concentration singularities. We show that such singular behavior occurs in our finite-depth system, and study the associated 3D flow structures.

DOI: 10.1103/PhysRevLett.112.128304

PACS numbers: 47.57.J-, 47.20.Ma, 68.03.Cd

Active fluids or suspensions have attracted much attention for their interesting, often unexpected dynamics [1]. Examples of active fluids include suspensions of microswimmers such as bacteria [2–4], or of chemically or optically driven particles [5–10], and complex networks of biopolymers and molecular motors [11,12]. These active soft materials differ from passive ones as they continuously consume energy from the surrounding environment to do work and are far from thermodynamic equilibrium, even in steady state conditions. This energy may come from chemical energy and the work done on the fluid can be used for self-propulsion. Most studies of active fluids have focused on suspensions of motile particles [1] whose active stresses, produced by swimming, and spontaneous flows can enhance mixing [13,14], and affect chemotactic aggregation (see Ref. [15] and references therein).

Here, we investigate a new type of active fluid with a different source of active stress. Consider immotile (non-swimming), but chemically active, particles that are bound to a flat surface sitting above a fluid layer [16–20]. These particles' activity creates (or depletes) a spatially diffusing chemical concentration field. At the surface, this chemical changes the local surface tension, and any consequent gradients in surface tension will produce Marangoni shear stresses. These “active” Marangoni stresses will produce fluid flows that move the particles. We call this surfing [21], and study it in the case of negligible fluid inertia and a chemical species whose transport is dominated by diffusion. Our theoretical analyses and simulations suggest that, if particle concentration raises surface tension (through the induced concentration field), surface flows of chemical surfers can yield large aggregations associated with vortical flows in the bulk. These might be harnessed for microfluidic manipulations [22,23] or flow assisted self-assembly [24,25].

Very surprisingly, we also show that for both sufficiently deep or shallow fluid layers the surface dynamics of particle density recovers the 2D parabolic-elliptic Keller-Segel (KS) model. Originally conceived to describe the chemotactically driven aggregation of motile slime molds, the KS model [26] is a canonical model of mathematical biology [27,28]. It describes the collective chemotactic dynamics of motile organisms that secrete and respond to a diffusing chemoattractant. KS dynamics can lead to aggregation and, under easily met analytical conditions, chemotactic collapse, which is an infinite pointwise density in finite time [27,28]. In the fluid dynamical context this collapse is associated with divergent velocity gradients and intense vortical structures.

That the dynamics of our system is, in certain limits, identical to the KS system is not obvious. However, the result derives from a very direct Fourier transform argument. This reveals an unexpected connection between self-attractive chemotaxis (termed “autotaxis”) of organisms and a purely physical fluid system driven by Marangoni stresses. In the following, we first describe how the dynamics of active particles is modeled followed by the derivation of the fluidic analogy to the KS model, and give results.

Consider a flat free surface, at  $z = 0$ , that sits above a layer of Newtonian fluid, of viscosity  $\mu$ , bounded by an impermeable solid wall at  $z = -H$  [see Fig. 1(a)]. Let  $\psi(\mathbf{x}, t)$  be the number density field of active particles on the free surface. The particles are carried passively by the surface fluid velocity  $\mathbf{U}(\mathbf{x}, t)$  and diffuse along the surface with diffusion constant  $D_p$ . Then,  $\psi$  satisfies

$$\psi_t + \nabla_2 \cdot (\mathbf{U}\psi) = D_p \Delta_2 \psi \quad (1)$$

in the  $z = 0$  plane where the subscript 2 denotes spatial derivatives in the  $\mathbf{x} = (x, y)$  plane. These particles are

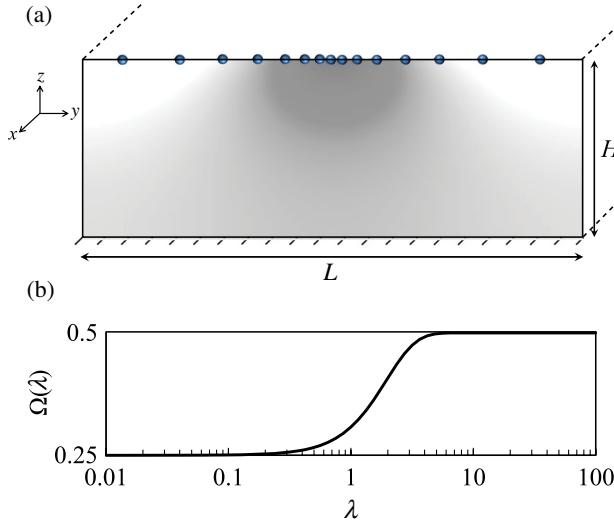


FIG. 1 (color online). (a) Schematic illustrating chemically active particles (dark circles) bound to a flat fluid surface sitting above a fluid layer of depth  $H$ . The gray-scale map represents the concentration field of the chemical species produced by the active particles. (b) Variation of  $\Omega$  as a function of  $\lambda$ .

chemically active and either deplete or produce a chemical species that diffuses into the bulk. Thus, the concentration field  $C(\mathbf{x}, z, t)$  of the chemical species satisfies

$$C_t + \mathbf{u} \cdot \nabla C = D_c \Delta C, \quad (2)$$

where  $D_c$  is a diffusion constant,  $\Delta$  is the 3D Laplacian in  $\mathbf{x}$  and  $z$ , and  $\mathbf{u}(\mathbf{x}, z, t)$  is the 3D fluid velocity. The flux boundary conditions of Eq. (2) are

$$D_c C_z(\mathbf{x}, 0, t) = \dot{m} \psi(\mathbf{x}, t) \quad \text{and} \quad C_z(\mathbf{x}, -H, t) = 0, \quad (3)$$

where  $\dot{m}$  is the rate of production ( $\dot{m} > 0$ ) or consumption ( $\dot{m} < 0$ ) of the chemical species per active particle.

The inertialess incompressible fluid flow with velocity  $\mathbf{u}(\mathbf{x}, z, t) = (u, v, w)$ , pressure  $p$ , and stress tensor  $\sigma = -p\mathbf{I} + \mu[\nabla\mathbf{u} + (\nabla\mathbf{u})^T]$  is driven by Marangoni shear stresses produced by surface gradients in  $C$ . We make the standard assumption that the surface tension  $\gamma$  depends linearly on the surface concentration of the chemical species [29,30], so that  $\gamma(\mathbf{x}, t) = \gamma_0 + \alpha C(\mathbf{x}, 0, t)$ , where  $\gamma_0$  and  $\alpha$  are constants. To determine the surface velocity  $\mathbf{U} = (u, v)|_{z=0}$ , we must solve the 3D Stokes equations

$$\nabla \cdot \sigma = -\nabla p + \mu \Delta \mathbf{u} = \mathbf{0} \quad \text{and} \quad \nabla \cdot \mathbf{u} = 0 \quad (4)$$

with the boundary conditions

$$\mu(u_z, v_z)|_{z=0} = \nabla_2 \gamma = \alpha \nabla_2 C, \quad w(\mathbf{x}, 0, t) = 0, \quad (5)$$

and no slip at  $z = -H$ .

We consider the coupled Eqs. (1)–(5) in a  $L \times L \times H$  domain  $V$  that is  $L$  periodic in the  $x$  and  $y$  directions. We

make these equations dimensionless by scaling particle density, length, chemical concentration, time, and velocity with, respectively, the average conserved particle density  $\bar{\psi}$ ,  $L$ ,  $\dot{m}\bar{\psi}L/D_c$ , advection time scale  $\tau = \mu D_c / \dot{m} \alpha \bar{\psi}$ , and  $L/\tau$ .

Assuming  $C(\mathbf{x}, z, 0) = 0$ , the integration of Eq. (2) over the volume and applying the boundary conditions, Eqs. (3), yields  $\bar{C}(t) = (\int C dV) / \bar{V} = t / (\delta Pe_c)$ , where  $\bar{V}$  is the domain volume,  $\delta = H/L$ , and  $Pe_c = \tau_c / \tau$  with  $\tau_c = L^2 / D_c$  being the time scale of diffusion of the chemical species. Letting  $C(\mathbf{x}, z, t) = \phi(\mathbf{x}, z, t) + \bar{C}(t)$ , Eq. (2) becomes

$$Pe_c(\phi_t + \mathbf{u} \cdot \nabla \phi) = \Delta \phi - \delta^{-1} \quad \text{for} \quad -\delta \leq z \leq 0. \quad (6)$$

Assuming  $Pe_c \ll 1$  and so neglecting the left-hand side,  $\phi$  satisfies a quasisteady Poisson equation (after an initial transient), which can be solved via 2D Fourier transform in  $\mathbf{x}$  (see the Supplemental Material [31]). This yields  $\hat{\phi}(\mathbf{0}, z) = z^2 / (2\delta) + z + \delta/3$  and

$$\hat{\phi}(\mathbf{k}, z, t) = (\coth k\delta \cosh kz + \sinh kz) \hat{\psi}(\mathbf{k}, t) / k \quad (7)$$

for  $k \neq 0$ , where  $\mathbf{k} = (2\pi n_1, 2\pi n_2)$  is the 2D wave vector with  $k = |\mathbf{k}|$  and  $n_1, n_2$  are integers. The surface gradient  $\nabla_2 \phi|_{z=0} = (i\mathbf{k}/k) \coth(k\delta) \hat{\psi}(\mathbf{k}, t) = \widehat{\mathcal{R}}_\delta[\psi]$  is a generalized Riesz transform [32].

Though slightly more complicated, Eq. (4) with boundary conditions (5) can again be solved via Fourier transform in  $\mathbf{x}$  (see the Supplemental Material [31]), which allows us to relate the surface velocity to the density of active particles,

$$\hat{\mathbf{U}}(\mathbf{k}, t) = (i\mathbf{k}/k^2) \Omega(k\delta) \hat{\psi}(\mathbf{k}, t) \quad (8)$$

for  $k \neq 0$ , where

$$\Omega(\lambda) = \coth \lambda (\sinh^2 \lambda - \lambda^2) / (\sinh 2\lambda - 2\lambda). \quad (9)$$

Note that  $\hat{\mathbf{U}}(\mathbf{k} = \mathbf{0}, t) = \mathbf{0}$ .  $\Omega$  has a simple structure: for  $\lambda$  small,  $\Omega \approx 1/4 + O(\lambda^2)$  whereas for  $\lambda$  large,  $\Omega$  approaches  $1/2$  exponentially fast [Fig. 1(b)]. That  $\Omega$  remains finite as  $\delta \rightarrow 0$  is interesting. While viscous dissipation increases with narrowing of the gap between the free surface and solid wall, the surface gradient of  $C$ , and therefore the driving Marangoni stress, increases with a decrease in  $\delta$  [see Eq. (7)]. These two effects cancel, which gives rise to a finite  $\Omega$  even when  $\delta$  is very small.

Hence, in both limits, Eq. (8) reduces to

$$\beta \hat{\mathbf{U}}(\mathbf{k}, t) = (i\mathbf{k}/k^2) \hat{\psi}(\mathbf{k}, t), \quad (10)$$

where  $\beta = 2$  (deep layer) or  $4$  (shallow layer). In real space we can write Eq. (10) as

$$\beta \mathbf{U} = -\Delta_2^{-1} \nabla_2 \psi, \quad (11)$$

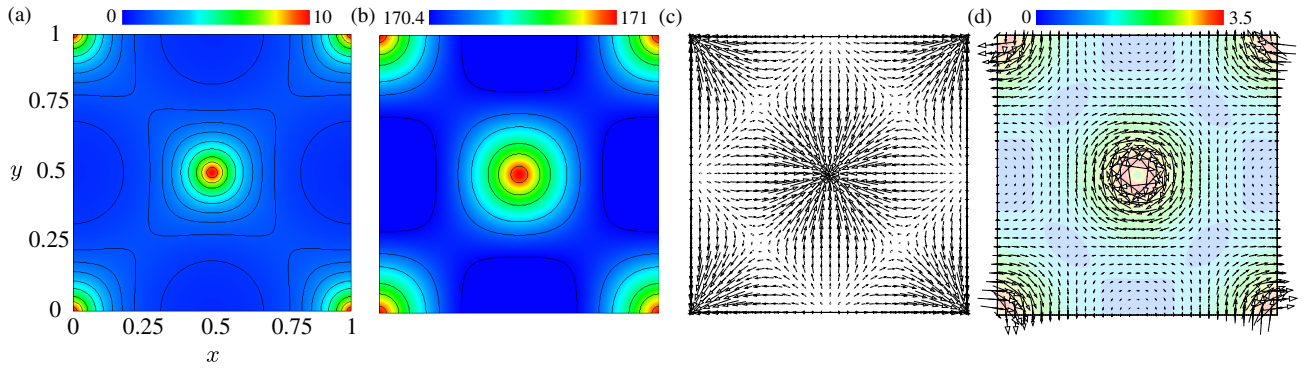


FIG. 2 (color online). For  $\delta = 1/2$ , contours of (a) particle density  $\psi$ , (b) chemical surface concentration  $C$ , and (c) the surface velocity field from Eq. (8). (d) The in-plane surface vorticity field  $\omega$  overlaid with a color map of vorticity magnitude  $\omega$ . The data correspond to  $t/t_c \approx 0.9$  where  $t_c$  is the estimated collapse time. Simulation parameters are  $\Delta t = 1/400$ ,  $\Delta x = \Delta y = 1/256$ ,  $Pe_c = 0.1$ ,  $Pe_p = 400$ , and  $\psi(\mathbf{x}, 0) = 1 + 0.1 \cos(2\pi x) \cos(2\pi y)$ . Vorticity is scaled by  $1/\tau$ .

and Eq. (1) becomes

$$\psi_t - \nabla_2 \cdot [(\psi/\beta)(\Delta_2^{-1} \nabla_2 \psi)] = Pe_p^{-1} \Delta_2 \psi, \quad (12)$$

where  $Pe_p = \tau_p/\tau$  with  $\tau_p = L^2/D_p$  the time scale of diffusion of active particles. Surprisingly, rescaling of Eq. (12) when  $\dot{m}\alpha > 0$  recovers the 2D parabolic-elliptic KS model for autotactic aggregation. This model is given by equations for the organismal density  $\varphi(\mathbf{x}, t)$  and the collectively produced chemoattractant concentration  $\rho(\mathbf{x}, t)$ ,

$$\varphi_t + \nabla_2 \cdot (\chi \varphi \nabla_2 \rho) = \Delta_2 \varphi \quad \text{and} \quad \Delta_2 \rho = -\varphi. \quad (13)$$

Read as a kinetic equation for conservation of species number, the first equation of Eqs. (13) states that the organismal speed is  $\chi \nabla_2 \rho$  with “chemotactic” strength  $\chi$ . The Poisson equation states that the chemoattractant is produced locally at a rate proportional to the organismal density, and is rapidly diffused. Its solution can be written formally as  $\rho = -\Delta_2^{-1} \varphi$ . Thus, the evolution equation for  $\varphi$  has the same form as Eq. (12). However, though  $\psi$  and  $\varphi$  are governed by the same equation, surface distributions of  $C$  and  $\rho$  are different since  $\Delta_2 C = \nabla_2 \cdot \mathcal{R}_\delta[\psi] \neq -\psi$ . Much is known about Eqs. (13). For instance, given a sufficient mass of organisms in the plane, the 2D KS model leads to chemotactic collapse in finite time [27,28,33,34]. The collapse singularity is approximately self-similar, i.e.,  $\varphi(\mathbf{x}, t) \approx \zeta^{-2} \Phi(|\mathbf{x}|/\zeta)$  for some function  $\Phi$  and a scale  $\zeta$  whose dominant algebraic part is  $\sqrt{t_c - t}$ , with  $t_c$  the collapse time [35]. In addition,  $\zeta \rightarrow 0$  and  $\varphi$  becomes a Dirac  $\delta$  function in  $\mathbf{x}$  as  $t \rightarrow t_c$ . See Refs. [27,28] for comprehensive reviews.

Consistent with this, linear stability analysis of Eqs. (1) and (8) shows that the system is unstable to 2D surface flows if  $Pe_p > 2/\Omega(\sqrt{2}\delta)$  as  $Pe_p$  scales linearly with  $\bar{\psi}$  (see the Supplemental Material [31]). In this scenario,

particle activity locally increases the surface tension ( $\alpha \dot{m} > 0$ ) and Marangoni stresses produce flows that concentrate the surface density of particles, leading to yet higher surface tension. Unlike the 2D KS problem, the surface flow in our system is associated with fully 3D fluid flow and structures.

We simulate Eqs. (1) and (8) using a semi-implicit, second-order in time, Fourier pseudospectral method for  $\dot{m}\alpha > 0$ . We set  $\psi(\mathbf{x}, 0) = 1 + 0.1 \cos(2\pi x) \cos(2\pi y)$  and fix  $Pe_p = 400$  which gives rise to instability independent of  $\delta$ . We observe a rapid accumulation of active surface-bound particles at the center and corners of the domain, where the initial concentration is peaked. Figure 2(a) shows a snapshot of  $\psi(\mathbf{x}, t)$  near the collapse time when  $\psi_{\max} = \psi(1/2, 1/2) \approx 10$ . Due to the similarity of patterns across  $\delta$ , we only show the results for the case of  $\delta = 1/2$ . We see an analogous, though broader, distribution for  $C$  on the surface [Fig. 2(b)]. Note that  $C$  is one derivative smoother than  $\psi$  [see Eq. (7)], and on the surface blows up more rapidly than  $\rho$  in the KS model as  $\psi$  collapses.

The increased active particle density is accompanied by fluid flow towards the blowup points [Fig. 2(c)]. This surface flow generates a 3D flow in the bulk. Figure 2(d) shows the in-plane vorticity field at  $z = 0$  overlaid with the contour map of its magnitude, which highlights the 3D nature of the velocity field. The out-of-plane vorticity is zero since  $\mathbf{U}$  is a 2D gradient [Eq. (8)]. To better understand the bulk flow, consider the  $\delta \rightarrow \infty$  case ( $\beta = 2$ ). Applying the incompressibility condition at  $z = 0$  gives [see Eq. (11)]

$$\nabla_2 \cdot \mathbf{U} = -w_z|_{z=0} = (1 - \psi)/2. \quad (14)$$

This suggests that the out-of-plane rate of strain directly inherits the structure of  $\psi$ , and so diverges with any collapse. Figure 3(a) demonstrates such a behavior where the surface flow creates a vortex ring just below the free surface. Though with a different strength and dimension, a

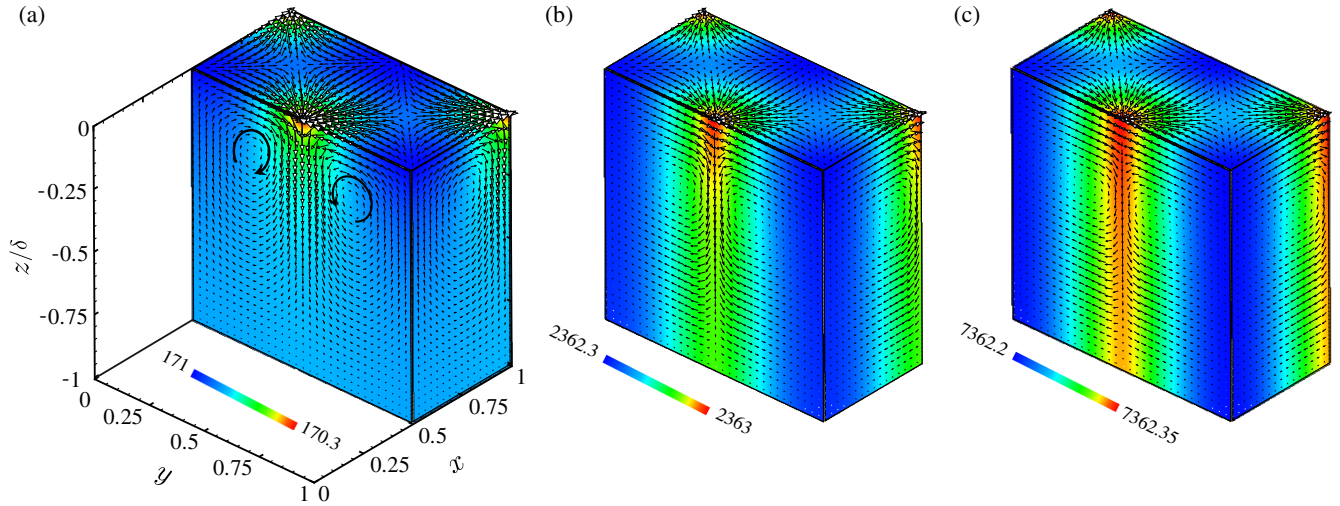


FIG. 3 (color online). The 3D velocity field overlaid with a color map of the chemical concentration  $C$ , at the time when  $\psi_{\max} = \psi(L/2, L/2) \approx 10$ .  $\delta = 1/2, 1/10, 1/20$  in (a), (b), and (c), respectively. Simulation parameters are the same as for Fig. 2. The  $z$  axis is scaled by  $\delta$ . The black arcs in (a) highlight vortical flows in the bulk.

vortex ring emerges in shallower fluid layers as well [see Figs. 3(b) and 3(c)].

Finally, we examine the effect of fluid layer depth on the putative collapse time. Figure 4 shows the divergence of  $\psi_{\max}$  for different values of  $\delta$ . We see that  $t_c$  increases with decreasing  $\delta$ , but remains finite for both deep or shallow layers. The collapse time is very well described by the shallow depth KS model for  $\delta \lesssim 0.01$  and by the infinite depth KS model for  $\delta \gtrsim 1$ . While the form of singularity in the asymptotic limits of  $\delta$  appears to be consistent with KS collapse, the precise nature of the apparent singularity for finite  $\delta$  is beyond the scope of this Letter.

Can our results be realized experimentally? The values for  $Pe_p$  and  $Pe_c$  used in our simulations can be realized in an aqueous system of size  $L \sim 100 \mu\text{m}$  and characteristic

fluid velocity  $L/\tau \sim 1 \mu\text{m/s}$ , using chemically active particles of radius  $R \sim 100 \text{ nm}$  that produce a chemical species with a diffusion constant  $D_c \sim 10^{-9} \text{ m}^2/\text{s}$ . Surface tension in this system is strong enough to keep the free surface flat. A challenge in developing such a system is designing a chemical reaction whose product increases the surface tension or whose reactants decrease the surface tension. Alternatively, an endothermic chemical reaction could increase surface tension by lowering the local temperature. Also, our results near the collapse time are not expected to be realized quantitatively since collapse leads to violation of many of our modeling assumptions such as finite velocity gradients, linearity of surface tension dependence on  $C$ , and large dynamic range of the surface tension (which, in reality, is small).

In this work, we considered active particles of isotropic shape that are much smaller than the characteristic size of the system. The use of anisotropic, or larger, active particles [16] could lead to other types of instabilities with different emerging flow patterns. Note that Marangoni stresses and associated 3D fluid flow in our system could be used for microfluidic manipulations [22] and directed self-assembly [24,25]. In fact, Marangoni stresses, induced by a chemical reaction, were utilized in a related system to create self-propelling liquid microdroplets [36]. It has been also reported that bacteria in biofilms exploit Marangoni stresses for dispersal [21], so it would be interesting to see whether any surface bound organisms take advantage of the Marangoni stresses for aggregation (say by consuming surfactant).

Lastly, we showed analytically that for sufficiently deep or shallow fluid layers the collective surfing of active particles is described by the iconic Keller-Segel model and we used the existing knowledge about its behavior to enhance our understanding of singularities in flow.

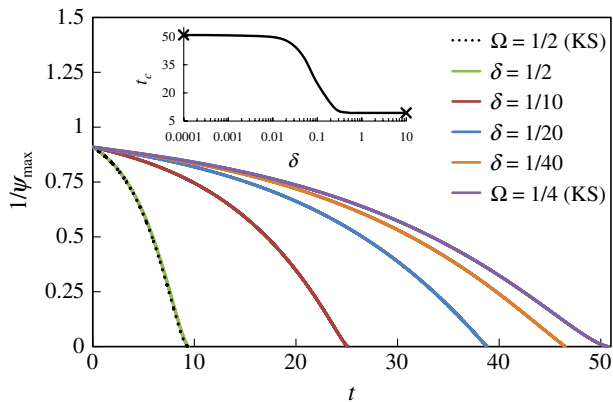


FIG. 4 (color online). Time variation of  $\psi_{\max} = \psi(1/2, 1/2)$  for different values of  $\delta$  and asymptotic cases of  $\Omega = 1/2, 1/4$  for which the evolution of  $\psi$  obeys the 2D KS model. The inset shows the variation of the estimated collapse time  $t_c$  as a function of  $\delta$ . Crosses show the asymptotic values of  $t_c$  for  $\Omega = 1/2, 1/4$ . Simulation parameters are the same as for Fig. 2.

Alternatively, it might prove fruitful to explore aspects of biological systems described by the KS model and its variants using chemically active particles that create active surface stresses for motion.

We thank J. Bedrossian, J. W. M. Bush, S. Childress, E. Nazockdast, L. Ristroph, and J. Zhang for useful conversations. H. M. and M. J. S. were supported by DOE Grant No. DE-FG02-88ER25053. H. M. acknowledges support from NSF Grant No. DMR-0844115 and the Institute for Complex Adaptive Matter. M. J. S. acknowledges support from NSF (NYU MRSEC DMR-0820341).

\*Hassan.Masoud@courant.nyu.edu

†shelley@cims.nyu.edu

- [1] D. Saintillan and M. J. Shelley, *C.R. Phys.* **14**, 497 (2013).  
 [2] A. Sokolov, I. S. Aranson, J. O. Kessler, and R. E. Goldstein, *Phys. Rev. Lett.* **98**, 158102 (2007).  
 [3] H. Wioland, F. G. Woodhouse, J. Dunkel, J. O. Kessler, and R. E. Goldstein, *Phys. Rev. Lett.* **110**, 268102 (2013).  
 [4] L. H. Cisneros, J. O. Kessler, S. Ganguly, and R. E. Goldstein, *Phys. Rev. E* **83**, 061907 (2011).  
 [5] W. F. Paxton, K. C. Kistler, C. C. Olmeda, A. Sen, S. K. St Angelo, Y. Y. Cao, T. E. Mallouk, P. E. Lammert, and V. H. Crespi, *J. Am. Chem. Soc.* **126**, 13424 (2004).  
 [6] Y. Hong, N. M. K. Blackman, N. D. Kopp, A. Sen, and D. Velegol, *Phys. Rev. Lett.* **99**, 178103 (2007).  
 [7] D. Takagi, A. B. Braunschweig, J. Zhang, and M. J. Shelley, *Phys. Rev. Lett.* **110**, 038301 (2013).  
 [8] J. Palacci, S. Sacanna, A. P. Steinberg, D. J. Pine, and P. M. Chaikin, *Science* **339**, 936 (2013).  
 [9] R. Golestanian, *Phys. Rev. Lett.* **108**, 038303 (2012).  
 [10] T. Bickel, G. Zecua, and A. Würger, [arXiv:1401.7833](https://arxiv.org/abs/1401.7833).  
 [11] T. Shinar, M. Mana, F. Piano, and M. J. Shelley, *Proc. Natl. Acad. Sci. U.S.A.* **108**, 10508 (2011).  
 [12] M. Sheinman, C. P. Broedersz, and F. C. MacKintosh, *Phys. Rev. Lett.* **109**, 238101 (2012).  
 [13] D. Saintillan and M. J. Shelley, *Phys. Rev. Lett.* **100**, 178103 (2008); *Phys. Fluids* **20**, 123304 (2008).  
 [14] A. Sokolov, R. E. Goldstein, F. I. Feldchtein, and I. S. Aranson, *Phys. Rev. E* **80**, 031903 (2009).  
 [15] E. Lushi, R. E. Goldstein, and M. J. Shelley, *Phys. Rev. E* **86**, 040902(R) (2012).  
 [16] H. Zhang, W. Duan, L. Liu, and A. Sen, *J. Am. Chem. Soc.* **135**, 15734 (2013).  
 [17] E. Lauga and A. M. J. Davis, *J. Fluid Mech.* **705**, 120 (2012).  
 [18] H. Masoud and H. A. Stone, *J. Fluid Mech.* **741**, R4 (2014).  
 [19] H. A. Stone and A. Ajdari, *J. Fluid Mech.* **369**, 151 (1998).  
 [20] H. A. Stone, *Phys. Fluids A* **2**, 111 (1990).  
 [21] T. E. Angelini, M. Roper, R. Kolter, D. A. Weitz, and M. P. Brenner, *Proc. Natl. Acad. Sci. U.S.A.* **106**, 18109 (2009).  
 [22] H. A. Stone, A. D. Stroock, and A. Ajdari, *Annu. Rev. Fluid Mech.* **36**, 381 (2004).  
 [23] H. Masoud and A. Alexeev, *Chem. Commun. (Cambridge)* **1** (2011) 472.  
 [24] M. T. F. Rodrigues, P. M. Ajayan, and G. G. Silva, *J. Phys. Chem. B* **117**, 6524 (2013).  
 [25] B. A. Grzybowski, H. A. Stone, and G. M. Whitesides, *Nature (London)* **405**, 1033 (2000).  
 [26] E. F. Keller and L. A. Segel, *J. Theor. Biol.* **26**, 399 (1970); **30**, 225 (1971); **30**, 235 (1971).  
 [27] D. Horstmann, *Jahresber. Dtsch. Math.-Ver.* **105**, 103 (2003).  
 [28] T. Hillen and K. J. Painter, *J. Math. Biol.* **58**, 183 (2009).  
 [29] W. E. Acree, *J. Colloid Interface Sci.* **101**, 575 (1984).  
 [30] W. F. Paxton, A. Sen, and T. E. Mallouk, *Chem. Eur. J.* **11**, 6462 (2005).  
 [31] See Supplemental Material at <http://link.aps.org/supplemental/10.1103/PhysRevLett.112.128304> for a detailed derivation of Eqs. (6–8) and the origin of the stability condition.  
 [32] G. F. Carrier, M. Krook, and C. E. Pearson, *Functions of a Complex Variable: Theory and Technique* (McGraw-Hill, New York, 1966).  
 [33] S. Childress and J. K. Percus, *Math. Biosci.* **56**, 217 (1981).  
 [34] S. Childress, *Chemotactic Collapse in Two Dimensions* (Springer-Verlag, Berlin, 1984), pp. 61–66.  
 [35] M. A. Herrero and J. J. L. Velazquez, *J. Math. Biol.* **35**, 177 (1996).  
 [36] S. Thutupalli, R. Seemann, and S. Herminghaus, *New J. Phys.* **13**, 073021 (2011).